PERGAMON

AVAILABLE AT
www.ComputerScienceWeb.com
POWERED BY SCIENCE DIRECT®

Neural Networks 16 (2003) 365–374

Neural Networks

www.elsevier.com/locate/neunet

2003 Special Issue

Ground-based telescope pointing and tracking optimization using a neural controller

D. Mancini, M. Brescia*,[1], P. Schipani

INAF-Astronomical Observatory of Capodimonte Via Moiariello 16, Napoli I-80131, Italy

Abstract

Neural network models (NN) have emerged as important components for applications of adaptive control theories. Their basic generalization capability, based on acquired knowledge, together with execution rapidity and correlation ability between input stimula, are basic attributes to consider NN as an extremely powerful tool for on-line control of complex systems. By a control system point of view, not only accuracy and speed, but also, in some cases, a high level of adaptation capability is required in order to match all working phases of the whole system during its lifetime. This is particularly remarkable for a new generation ground-based telescope control system. Infact, strong changes in terms of system speed and instantaneous position error tolerance are necessary, especially in case of trajectory disturb induced by wind shake. The classical control scheme adopted in such a system is based on the proportional integral (PI) filter, already applied and implemented on a large amount of new generation telescopes, considered as a standard in this technological environment. In this paper we introduce the concept of a new approach, the neural variable structure proportional integral, (NVSPI), related to the implementation of a standard multi layer perceptron network in new generation ground-based Alt-Az telescope control systems. Its main purpose is to improve adaptive capability of the Variable structure proportional integral model, an already innovative control scheme recently introduced by authors [Proc SPIE (1997)], based on a modified version of classical PI control model, in terms of flexibility and accuracy of the dynamic response range also in presence of wind noise effects. The realization of a powerful well tested and validated telescope model simulation system allowed the possibility to directly compare performances of the two control schemes on simulated tracking trajectories, revealing extremely encouraging results in terms of NVSPI control robustness and reliability.

Keywords: Telescope; Tracking; Adaptive control system; Neural network; Multilayer perceptron; Back propagation

1. Introduction

During an astronomical observation, the main telescope operations are pointing (reaching the target object) and tracking (following the object during its apparent motion). These phases are executed in sequence without a well-defined transition phase between them. The whole collect of astronomical data is performed along tracking. This makes tracking the most important phase during an entire object observation cycle. During this phase there is a slow dynamical coupling of the two main axes (azimuth and altitude). The altitude axis stops its motion when crosses the meridian, while the azimuth axis increases its velocity, near the zenith up to about $1000''$/s. Furthermore, wind buffeting on telescope structure introduces a considerable disturb, especially on altitude axis. As a consequence the speed dynamic range is about 40 db, with a RMS tolerable error not greater than $0.15''$ in order to guarantee an optimal image quality during the observations. The optimal image quality can be guaranteed only by maintaining the total telescope tracking RMS error lower than arcsec/pixel resolution, induced by technical features of the instrument charge coupled device (CCD) mounted on the telescope. This makes evident the strong dynamic changes of control requirements. It will be desirable to have a control system able to modify dynamically its response, in terms of its parameters variation, in order to match exactly the whole system dynamic range and to follow the tracking trajectory without affecting the observation performance.

2. Control design

During telescope control system development, error analysis is one of the most careful aspects to take into account. In this context, errors can be classified as

* Corresponding author. Tel.: +39-81-5575553; fax: +39-81-5575563.
E-mail address: brescia@na.astro.it (M. Brescia).
[1] URL: http://www.maxbrescia.it

0893-6080/03/$ - see front matter © 2003 Elsevier Science Ltd. All rights reserved.
doi:10.1016/S0893-6080(03)00023-6

systematic and random errors. In the first case, using appropriate lookup tables (LUT), it is possible to identify and to correct this kind of errors. In the latter case, the presence of random effects, such as ball bearing rolling errors or wind shake as well, affects the axes instantaneous position and it depends from system actual speed (Mancini, Brescia, Cascone, & Schipani, 1997). It is clear that a dependence of control parameters from axes speed is needed. Unfortunately, this dependence of noise effects from speed cannot be systematically identified, due to their random nature. The random error correction capability depends only by intrinsic control system adaptive nature.

2.1. Standard approach: static control structure

In the classical approach, the control design methodology, based on a unique controller able to satisfy all the above demands in all system working phases, has the limit that it cannot guarantee the required precision in all working phases. For example, a classical PI structure can introduce additional noise, (system oscillation and instability), when its integral action is employed in presence of a high error trend. Doing so, it is impossible to respect all required demands for both pointing and tracking phases. On the other hand the dynamic use of different controllers in sequence can introduce noise during transition between themselves, generating discontinuities during the most careful working phases of the telescope. Furthermore, an optimized controller for tracking phase, in presence of low position errors, would have some problems in case of unexpected error variations due to external stimula, such as wind buffeting. Therefore the natural evolution of a controller able to outcome all the limits of the above models is represented by developing a control system able to perform a self-tuning of its parameters according to different working phases. Doing so, it will be possible to avoid either problem related to the transitions between different controllers and to the presence of unexpected position error variations. Such a controller would be able to adapt self-parameters according to position error, axis position and speed as well. A typical example of such a controller is the PI + anti windup (PI + AW), (Fig. 1), where there is not a real variability in terms of its parameters but rather the use of the anti windup device able to increase the performance in case of system actuators saturation. Unfortunately,

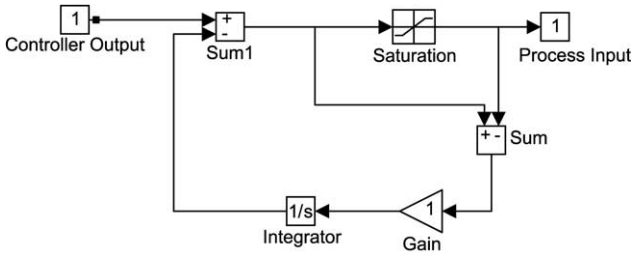

Fig. 1. PI + AW control scheme.

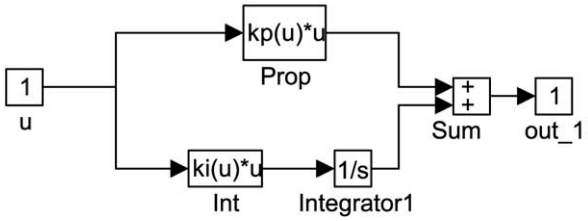

Fig. 2. VSPI control scheme.

this kind of controllers has not the versatility level required by our control system.

2.2. Innovative approach: variable structure controller

In Mancini et al. (1997), we proposed a VSPI, (Fig. 2), able to correct the problem of actuators saturation and able to adapt itself to different variations of position instantaneous error.

The laws related to the classical PI and to our VSPI model are as follows

$$y = k_p e + k_i \int e \, dt \text{ (classic PI)}$$
$$y = k_p e + k_i(e) \int e \, dt \text{ (VSPI)} \tag{1.1}$$

$$k_p = \frac{k_{op}}{1 + c_p |e|^n} \qquad k_i = \frac{k_{oi}}{1 + c_i |e|^m} \tag{1.2}$$

The VSPI scheme represents a more versatile solution, where both the integral and proportional actions are weighted on the position instantaneous error value. The controller's parameters are therefore variable, making the controller itself able to optimize its performance in all working phases. The limit of this approach is that the parameter's variation law is one-dimensional, depending only on the position instantaneous error, without taking into account other system parameters variation, able to modify global system behavior. Furthermore it does not represent a self-adaptive control system, because there is not a direct feedback on the dynamic parameter variations. It would be desirable to introduce in the control system a tool able to 'observe' the global system behavior and related control subsystem action, to 'analyze' in real time the accuracy level of controller response and to 'operate' in order to optimize the performance. These considerations are the basic concepts deriving the decision to investigate an approach based on the introduction of a neural network in the control system, starting from the statement that such a tool makes of the self-adaptation its main dowry.

3. VSPI optimization with neural network

Fixed structure controllers have shown a weakness in optimizing the telescope performance in terms of position

error amount in the whole required dynamic range. On the contrary a variable structure controller, with the ability to modify itself during operations, according to the instantaneous error values, has reached the best global performance in the case of a sophisticate system where tracking noises are reduced by means of a good system design (Mancini et al., 1997). A more sophisticated control, taking into account system status, actual speed and characterization, could be necessary for systems where torque noise problems could arise during the system lifetime itself, such as bearing and gear consumption or dust, or in the case of high frequency perturbations, such as wind buffeting. Usually the resulting errors are due to the inability of a PI based controller to respond in time. In order to improve the control system speed performance, an observer, based on a neural network, can be added to the VSPI controller in order to impose high frequency torque offsets directly to the power amplifier without affecting the VSPI control still devoted to system stabilization. In practice, an element known in the control system theory as a feed-forward gain, but able to adapt itself to instantaneous system requirements.

3.1. The NN model: multilayer perceptron

A particular class of networks which has received considerable attention in the area of artificial neural networks is multilayer perceptron (MLP). A typical MLP model structure can be denoted in block diagram form as shown in Fig. 3 with three weight matrices U, V and W, (Miller, Sutton, & Werbos, 1990). The multilayer network represents a nonlinear map f( ) where $o = f(x) = F[WF[VF[Ux]]]$ and the elements of U, V and W are adjustable weights.

Such networks have been used successfully in pattern recognition, where the weights are adjusted to minimize a suitable error function. From a system-theoretical point of view, the multilayer network represents merely a versatile nonlinear map. In our approach we will use such a neural network as a subsystem encapsulated into the VSPI control system. First of all, it is necessary to address the following problem: if NN are introduced for control purpose in dynamic systems, their approximation capabilities must be well understood when a finite number of layers with a specified number of nodes in each layer is present in the network (Fig. 4).

In particular, all network inputs chosen must guarantee a correlation between them to be useful for feature learning by the network. This will assure that the control problem is well posed. In Section 3.1 we shall discuss our approach to achieve this concept in our model. The adjustment of the weights of

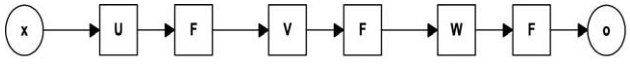

Fig. 3. Block diagram of a three layer neural network.

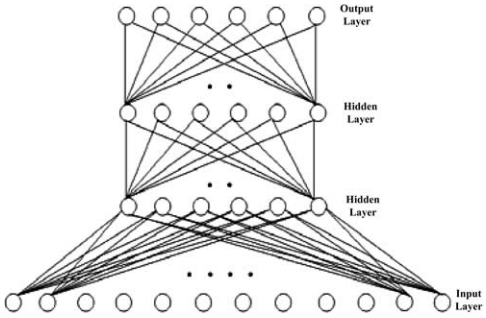

Fig. 4. MLP architecture.

the NN, when the latter is used as a component in a dynamic control system, can be considered as the adaptive part (the brain) of the control process needed to improve performance in terms of optimal response in a wide bandwidth to the input signal. Back propagation (BP) is one of the computationally efficient methods for the adjustment of the weights of specified NN models. In such a method, the partial derivatives of an error criterion as regards the weights in a MLP are determined and the weights in turn are adjusted along the negative gradient to minimize the error function. The structure of the weight matrices used to compute the derivatives is seen to be identical to that in the original network, while the signal flow is in the opposite direction (this justifies the term BP). This concept is also strongly related to the powerful concept of feedback in the control system theory. In the classical approach the neural control architecture is based on a control subsystem represented by a NN and a reference model that can be realized either by a specialized NN or any classical identification model. The control law is then based on comparison between reference model and controlled system output. In particular two distinct approaches to the adaptive control are normally used, (Miller et al., 1990): direct control, where the parameters of the controller are directly adjusted to reduce some norm of the output error, and the indirect control, where the parameters are estimated at any time instant and the parameter vector of the controller is chosen assuming that the estimation represents the true value of the plant parameter vector.

3.1.1. First classical neuro controller approach: direct adaptive control

In conventional direct adaptive control theory, methods for adjusting the parameters of a controller based on the measured output error rely on concepts such as correlating the two signals, respectively, reference model signal and controlled system one. At present there are not well fixed methods for directly adjusting the parameters of the neural controller (Miller et al., 1990). This is due to the nonlinear nature of both the system and the controller. Also, BP cannot be used directly, since the exact system reference model is unknown and hence cannot be used to generate the desired partial derivatives. The basic direct adaptive control architecture is illustrated in Fig. 5.

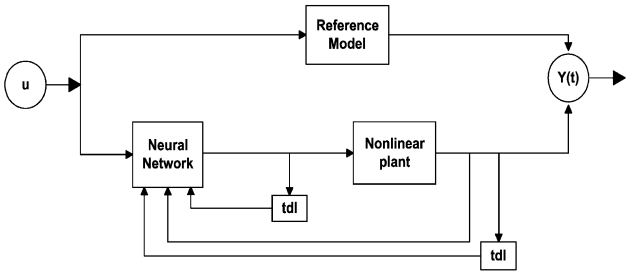

Fig. 5. Direct adaptive control using neural networks.

3.1.2. Second classical neuro controller approach: indirect adaptive control

When indirect adaptive control is used to control a nonlinear system, the model parameters are updated using the identification error. The controller parameters are adjusted by back propagating the error between the identified model and the reference model outputs through the identified model, (Miller et al., 1990). A block diagram of such an adaptive system is shown in Fig. 6.

Both identification and control can be carried out at every instant or after processing the data over finite intervals. When external noise is present, identification is carried out at every instant while control parameter updating is carried out over a slower time scale, to assure robustness of the system performance. Limits of the latter model are that the specified model used to identify the system depends critically on the prior information available. Also in the two approaches described earlier is tacitly assumed that the reference model is linear.

3.2. Innovative neuro controller approach: NVSPI model

Our approach in the control system architecture can be considered hybrid, in the sense that it combines the control design approaches seen before, (VSPI + NN = NVSPI), to obtain an optimized adaptive control system, able to correct telescope axes position in case of unpredictable and unexpected position errors. The control main device is the VSPI structure mentioned earlier that, during default operative conditions, (low position errors), and also in case of limited increase of error conditions, is able to carry out the optimal corrections needed. When the increase of the error or any unexpected wrong condition occurs, the VSPI is not able to completely correct the system performance. To prevent such critical events, we provide an additional tool, working with the VSPI, able to introduce an additional term in the control law input to the system in order to correct the error. This additional tool is a NN, representing the adaptive self-tuning capability of our control system structure.

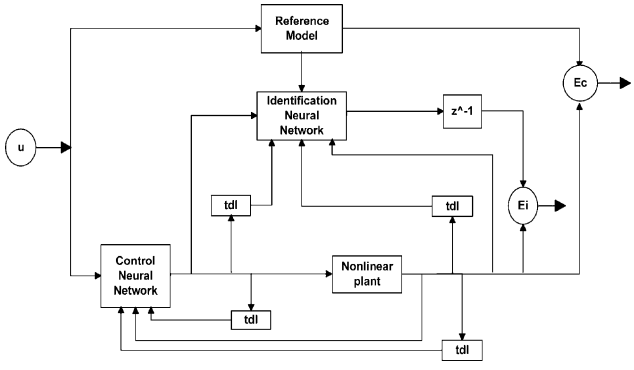

Fig. 6. Indirect adaptive control using neural networks.

3.2.1. NVSPI learning architecture

Fig. 7 illustrates the NVSPI control architecture during the off-line learning phase. Using a MLP network with BP learning algorithm, this phase consists of a serial presentation of a learning set of input–output data couples (reference position trajectories in this case) through the system in order to teach the NN to recognize fault condition of the VSPI response. The learning phase diagram is shown in Fig. 7.

In desired conditions, input reference position U and output actual position Y should be the same. The presence of noise introduces an error term $e = Y - U$. This term represents the input of the VSPI. The latter, laws (1.1) and (1.2) generate the output $P(e)$ that is one of the NN inputs, together with the position error term e and the system reference position input U. Through the forward part of the BP algorithm the NN gives its output $N(U, e, P(e))$. The laws related to the forward part of BP algorithm are

$$\text{net\_input}_h = \sum_i W_{hi} O_i \tag{3.1}$$

$$\text{net\_input}_j = \sum_h W_{jh} O_j \tag{3.2}$$

$$f(0) = \frac{1}{1 + \exp(-0)} \tag{3.3}$$

$$N(U, e, P(e)) = \frac{1}{2k} \sum_j (Y_j - P(e))^2 \tag{3.4}$$

where the terms mean

U	system reference position input;
Y	system actual position output;
e	VSPI input (position error);
$P(e)$	VSPI output (system required position);
O_i	NN input $(U, e, P(e))$;
O_h	input of the NN output layer;

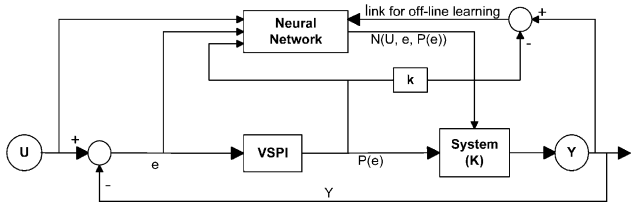

Fig. 7. NVSPI off-line learning control scheme.

net_input$_h$ global input of generic hidden layer;
net_input$_j$ global input of the NN output layer;
$f(0)$ neuron activation function;
$N(U, e, P(e))$ N output function;

The formula (3.4) is normalized with a constant coefficient k, representing the system coefficient and added to the $P(e)$ term. This sum is the input to the system to be controlled. Finally the system output Y is compared with the $P(e)$ term, (3.9), to evaluate the performance of both VSPI and NN and this difference is back propagated through the NN, using the backward part of the BP algorithm, to adjust the weight matrix of the network along the steepest descent of the error gradient. Below laws for this part of the BP algorithm are shown

$$\delta = f'(0)(Y - P(e)) \tag{3.5}$$

$$\delta'' = f'(0)\sum w\delta \tag{3.6}$$

$$w_{ji}(\text{new}) = w_{ji}(\text{old}) + \eta\delta_i o_j + \alpha\Delta w_{ji}(\text{old}) \tag{3.7}$$

$$Y = k\left[P(e) + \frac{1}{k}N(U, e, P(e))\right] \tag{3.8}$$

$$|Y - P(e)| < \varepsilon \quad \text{NN learning criterium} \tag{3.9}$$

where the terms mean

ε little constant a priori fixed;
δ output layer delta function;
δ'' hidden layer delta function;
w_{ji}(new) weight updating law;
η learning rate;
α momentum factor;
k system coefficient;

This phase ends when the difference between Y and $P(e)$ is smaller than a little fixed constant. The choice of the NN input space is based on the consideration that both system input U and error term e are trivially correlated and together give information needed about system state. Furthermore, third term $P(e)$, VSPI output gives information to the net about VSPI response in terms of its parameters and its level of correction input for the telescope axes. Finally, based on system against VSPI response, the NN will be able to understand the correlation between its behavior, system performance and VSPI response and will carry out internal adaptation adjusting its own weight matrix, in order to give a better response at the next output. From a practical point of view, a slow learning will be needed, in terms of weight adjustment and learning rate and momentum factor choices, together with a not too small error constant ϵ fixed, in order to perform a better generalization during on-line working.

3.2.2. NVSPI on-line architecture

In Fig. 8 it is shown the block diagram of our final control system after NN learning phase. At this time all basic choices about NN parameters, (i.e. number of hidden layers, number of hidden and output nodes, best values of learning rate η and momentum factor α), are fixed.

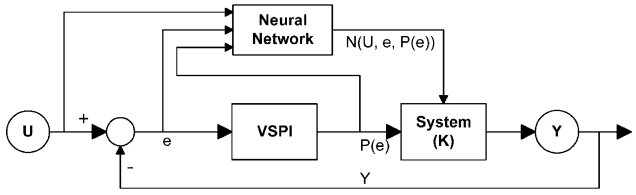

Fig. 8. NVSPI on-line control scheme.

If the training set data used has been appropriate, in terms of number and quality of samples, the net will be able to carry out its better generalization on both validation and input test data sets. In particular, the net contribution will be proportional to the response level of the VSPI, adding to $P(e)$ the best value in order to dynamically correct system behavior. This feature gives to the NN a role of a typical observer of the control flow, able to modify, if needed, the control contribute to the main system. The net, infact, controls VSPI performance directly during both off- and on-line working phases, and system performance directly in the off-line phase and indirectly during on-line phase.

3.3. The NVSPI experiment

In order to test and verify the goodness of NVSPI theoretical investigation in a sense of a better tracking control, we have carried out an experiment on a real telescope model, by comparing tracking performances between VSPI and NVSPI solutions. In the following, best results are reported and discussed, together with a brief description of the telescope model used.

3.3.1. The telescope system model

In this section it is introduced a brief description of the telescope system model, realized in order to represent the black box 'System' as shown in scheme of Figs. 7 and 8. Details of the system model are beyond the scope of the present study and are referred to specific papers (Schipani, 2002; Schipani, Brescia, Mancini, Marty, & Spirito, 2001). A real implementation of the control system block has been obtained by modeling the VST (VLT survey telescope), an Alt-Azimuthal 2.5 m telescope actually under integration by our group, planned to be located in the European Southern Observatory (ESO) very large telescope (VLT) observatory facility at Cerro Paranal, Atacama desert, Chile. It is a survey wide field imaging instrument, with a corrected field of view (FOV) of 1 squared degree, basically used to furnish a well defined target observational map for the VLT, the largest ground-based telescope in the world, (Schipani et al., 2001). The model has been obtained by means of the mechanical design and finite element analysis data and a simulation in time and frequency domains has been performed in order to evaluate its tracking performance in perturbed conditions, mainly due to wind shake. As usually

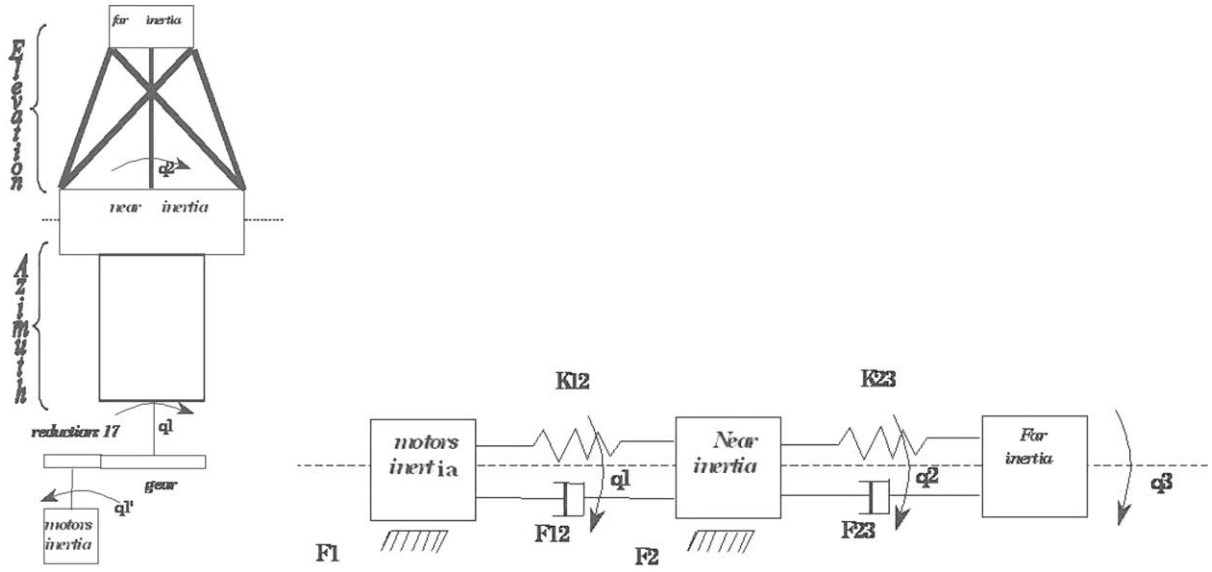

Fig. 9. Telescope model (main axes) block diagrams.

applied in telescope modeling, the structure is organized by modeling the two main axes (azimuth and altitude) by a number of inertias joined by stiffnesses and structural dampings.

The axis gear is represented by the motor and teeth contact stiffness and damping,. Four motors per axis are used in a symmetrical configuration, implementing a preload scheme which makes negligible the gear backlash. Also the motor inertia is taken into account, properly scaled by the transmission ratio. The dynamic of the mechanical system can be summarized by 2nd order differential equations in matrix form as

$$J\ddot{\Theta} + F\dot{\Theta} + K\Theta = T$$

where J, F, K, T are the inertia, viscous damping, stiffness and torque matrix, respectively, and Θ is the angular position vector. The speed and position controllers have to be tuned to guarantee the two most important requirements: an extremely low tracking error and a good disturbance rejection. The absolute RMS tracking error must be as low as possible in order to guarantee the image quality during the observations. Furthermore, the stability robustness of the closed loop must be guaranteed with proper gain and phase margins, to reject structural parameter changes of the controlled system and/or environment modifications. The main external disturbance to consider in this analysis is the wind shake. The wind mainly affects the altitude performance, because the altitude axis is subjected to a greater wind torque. The azimuth rotation is much more protected by the co-rotating enclosure. The site chosen for VST is sometimes windy. Therefore a wind effect analysis has been carried out in the following taking into account the Chilean site weather statistics. The azimuth axis in an Alt-Az telescope can assume very high speeds when altitude axis is close to zenith, especially when crossing the meridian, where the speed reaches its maximum. On the contrary when altitude angle is low, azimuth moves very slow (Schipani et al., 2001) Fig. 9. Therefore the position control can be difficult for azimuth, since the dynamic speed range is wide. The same thing does not apply to altitude axis, whose speed range is bounded up to a low value depending on the latitude of the site: for VST the maximum speed is about 13 arcsec/s.

3.3.2. NVSPI vs. VSPI test using wind disturbance analysis

In this analysis a VSPI has been used as speed and position loop controllers, which ideally guarantees zero error to a ramp input (similar to the usual real observation conditions) after the transient phase (i.e. from pointing to tracking). This is a little bit different from the classical control scheme adopted in telescope main axis servo systems, where a static PI controller is used, adding Notch filters at specific frequencies. The use of VSPI has been successfully implemented limiting the investigation to 'small' error case (i.e. to the tracking phase control). This choice reduces the complexity of the model simulated. Details of Simulink models used for simulation are described in Schipani (2002). Then we have applied the same tracking conditions to NVSPI system, by comparing tracking error results, as detailed in the following. A ground-based telescope works in open air and is only partially protected by a co-rotating enclosure, so the main external disturbance to the axes control system is certainly the wind. Therefore, the performance of a telescope position control servo system depends on its ability to minimize changes in position due to the wind. The altitude axis is certainly the most influenced by the wind disturbance and so most of the analysis will be focused on it. An approach to evaluate

Table 1
Simulation data

α	I	L (m)
1	0.15	79
0.98	0.15	3.2
0.63	0.12	3.2

the effect of the wind on the telescope performance is based on the description of the power spectral density of the wind by the Von Karman spectrum

$$S_v(f) = 4(Iv)^2 \frac{L}{v} \frac{1}{\left(1 + 70.78\left(f\frac{L}{v}\right)^2\right)^{5/6}}$$

where v is the mean wind speed, I is the turbulence intensity, f the frequency, L the outer scale of turbulence. Three simulations have been carried out with the data shown in Table 1 (where α is a wind speed reduction factor).

These data refer to three different conditions: $\alpha = 1$, i.e. no wind speed reduction, shows the extreme situation of the telescope completely in open air; $\alpha = 0.98$ refers to the not favorable situation of the telescope observing in the direction of the wind, a scenario usually avoided whenever possible in real observations; $\alpha = 0.63$ refers to a more realistic situation of the telescope properly protected by the enclosure and some wind screens. The wind speed range used in the simulation has been chosen up to $v = 18$ m/s; over this value no observation is usually performed in the ESO Cerro Paranal observatory. The wind presence problem anyway should be limited to a low percentage of telescope usage time; the wind speed is above 12 m/s in about 11% of the time, above 15 m/s only in the 5% of the time (Fig. 10).

The PSD of the altitude axis rotation due to the disturbance torque (Fig. 11) can be obtained by multiplying the spectrum modified by the introduction of aerodynamic correction factor (Schipani, 2002), with the square of

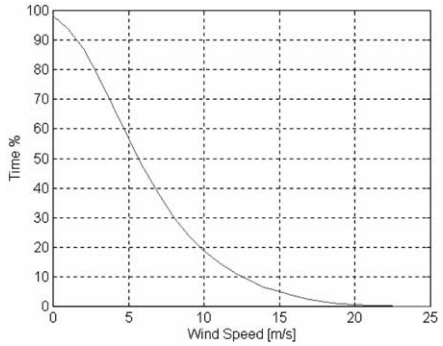

Fig. 10. Time% vs. wind speed in Paranal.

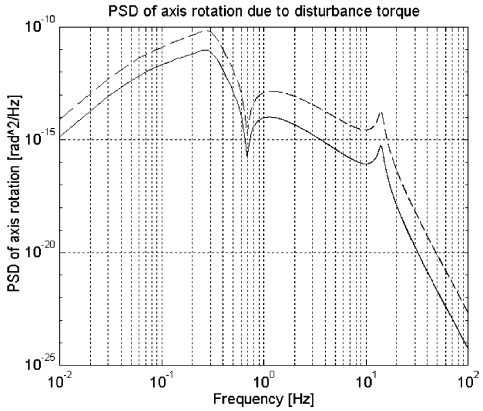

Fig. 11. PSD of axis rotation due to the wind disturbance torque $S_\theta(f)\times$ ($\alpha = 0.98$ dashed line, $\alpha = 0.63$ continuous line).

the disturbance transfer function $D(f)$

$$D(f) = \frac{\theta(f)}{\tau(f)}$$

$$S_\vartheta(f) = |D(f)|^2 S_\tau(f)$$

The amplitude of the disturbance as calculated with this approach depends on data mutuated from VLT wind tunnel tests and related experience. The RMS displacement error due to the torque disturbance induced by the wind is represented as a function of the bandwidth of the control loop in Fig. 12.

Most of the disturbance effect is concentrated below 1 Hz. Higher the bandwidth, better is the disturbance rejection; in practice the bandwidth is limited by the dynamic of the telescope, mainly by the locked rotor frequency. The bandwidth estimated for VST is about 3 Hz, sufficient to contrast effectively the wind disturbance. Better error estimation is obtained from the time domain analysis reported in the following.

The wind disturbance effect has been studied, for both VSPI and NVSPI cases, in the time domain simulating

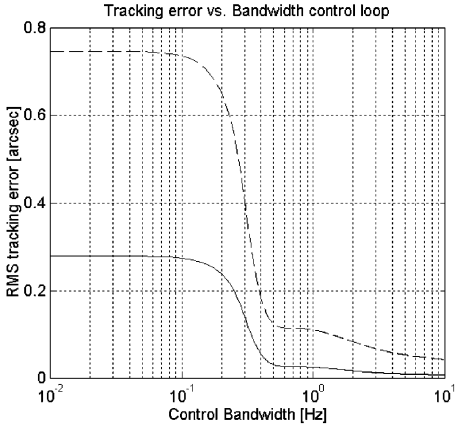

Fig. 12. Tracking error vs. bandwidth of the control loop ($\alpha = 0.98$ dashed line, $\alpha = 0.63$ continuous line).

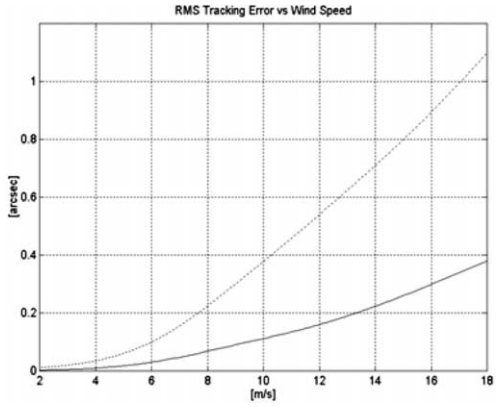

Fig. 13. Control model RMS tracking error vs. wind speed ($\alpha = 0.63$ case) (VSPI upper line, NVSPI lower line).

Table 2
NVSPI neural network experiment main parameters

NVSPI experiment parameter	Value
Input nodes	3
Hidden nodes level 1	5
Hidden nodes level 2	3
Output nodes	1
Best learning rate	0.07
Best momentum factor	0.23
Training patterns (trajectories pre-calculated)	1000
Test patterns (used for validation and comparison with VSPI)	100
Training and test pattern time duration	50 s
Altitude axis angle range used for training and test patterns	30–80

a tracking at a speed of 10 arcsec/s (almost the maximum velocity for altitude), generating torque disturbance time series as a sum of sine waves with amplitudes determined from the power spectral density and with random phases (Andersen, 1994)

$$\tau(t) = \sum_{1}^{N} \sqrt{2S_\tau(f_k)\Delta f}\cos(2\pi f_k t + \phi_k)$$

where $\Delta f = 0.01$ Hz is the frequency resolution, $N = 10000$ the number of frequency samples, ϕ_k random phase angles. Two case studies have been considered ($\alpha = 0.63$, $\alpha = 0.98$), skipping the not realistic 'open air' condition ($\alpha = 1$) used before only for comparison. Two sets of simulations have been carried out at increasing wind speeds. It should be considered that since observing in the direction of the wind is not a preferred scenario the $\alpha = 0.63$ case can be considered the more realistic observation condition, having properly set the wind screens and the whole enclosure. The interpolation of the NVSPI vs. VSPI data results is reported in Fig. 13.

In the following we report test results obtained by comparing tracking performances in both VSPI and NVSPI models, applied to the more realistic case of wind disturbance ($\alpha = 0.63$). In the more negative case, ($\alpha = 0.98$), both models respond with approximately the same behavior, showing an expected high disturb to telescope tracking performance in pessimistic conditions where almost no wind disturbance reduction is achieved and the observations are done in the wind direction. The conditions created in the simulation are referred to the case of a simplified telescope control model in presence a good wind speed reduction inside the enclosure, thanks to a proper setting of wind-screens and not observing in the wind direction. Both control schemes have been applied to a simulation data set composed by an input trajectory, obtained by an astrometry loop, to be followed by the telescope model in time windows of 50 s.

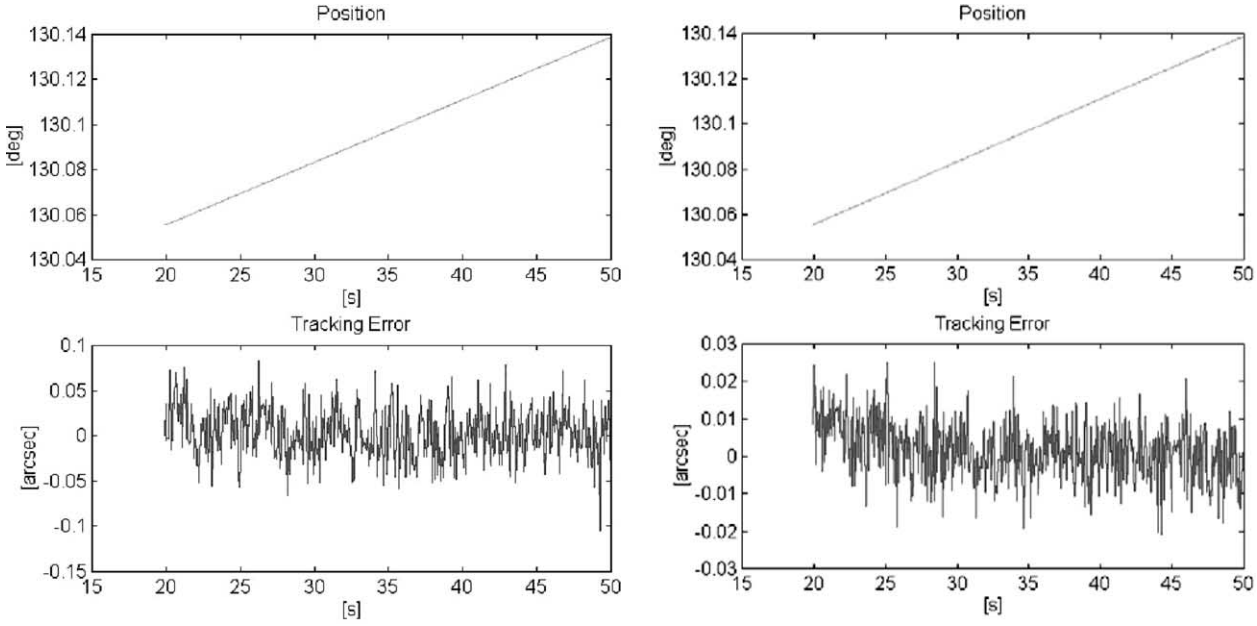

Fig. 14. Azimuth axis test. Tracking RMS result using VSPI (left figure) and NVSPI (right figure).

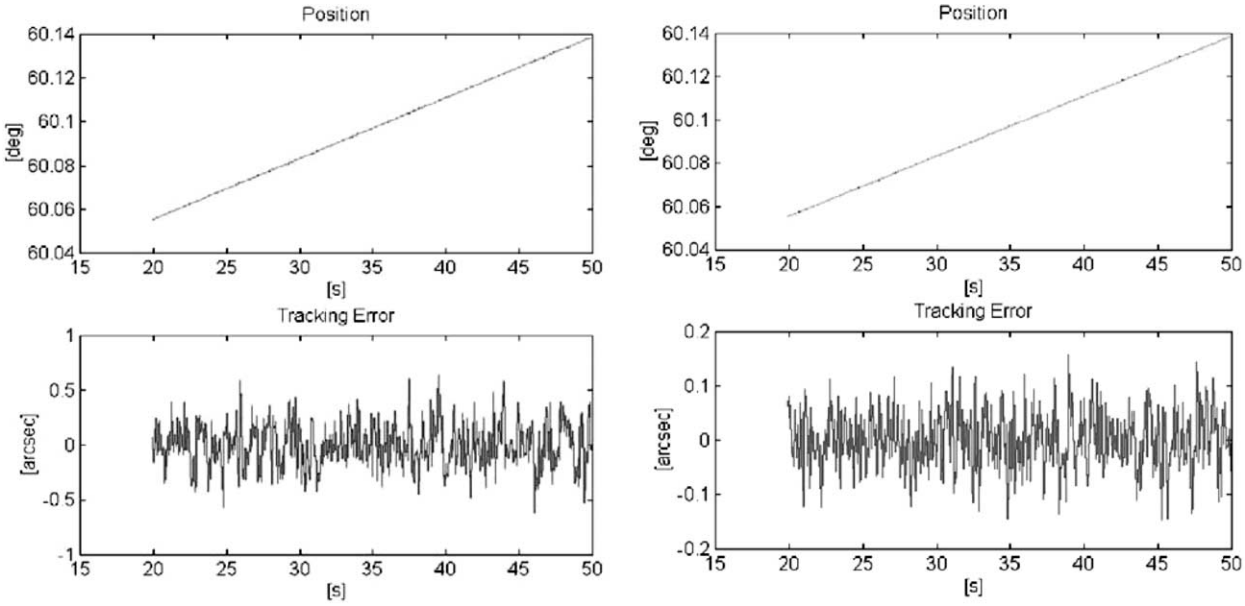

Fig. 15. Altitude axis test. Tracking RMS result using VSPI (left figure) and NVSPI (right figure).

The training set for the NVSPI has been organized by means of 1000 several trajectories, of the same time length and at different altitude ranging from 30 to 80 elevation degree. During input data presentation the wind disturbance ratio was introduced according the law described earlier. The learning phase has not been organized in the classical batch algorithm (weight adjustment after a complete training set presentation), but in the form of weight adjustment on single input pattern. This strategy has been conditioned by the NVSPI internal structure and learning data composition rule. The test set has been composed by trajectories of the same time length, with different altitude degrees (partially belonging to original training set). In Table 2, only the network and learning phase parameters, obtaining best performance, are listed.

The best results obtained, by comparing models implementing VSPI and NVSPI, respectively, have been obtained with above network parameters and, in particular, the figures reported below are referred to the best experiment results for test trajectory set for azimuth and altitude. In the first scheme of each figure showed, for each figure, the input trajectory is reported (axis position/time duration), while the second one shows the RMS tracking error obtained during tracking simulation, expressed as arcsec/s. For the azimuth axis, (Fig. 14), both VSPI and NVSPI control schemes are able to maintain reference trajectory displacement well under the system requirements (<0.21 arcsec), as already expected from the low disturb induced by wind on this axis, though there is a strong evidence of a better behavior of the NVSPI control scheme in terms of axis stability and quick reaction to wind shake.

In the case of altitude, Fig. 15, the NVSPI control scheme seems to react essentially better than VSPI model, maintaining RMS error under 0.16 arcsec against 0.54 arcsec obtained by VSPI model. The high capability of the NVSPI to introduce a very quick reaction to wind shake displacement gives to the neural network a role of an adaptive feed-forward gain in the control system architecture. The encouraging results obtained by such a neural control model show the possibility to obtain high control performances as result of a not very complex optimization process of classical PI filter, making it comparable with modern more complex control schemes, also in case of a quasi real time control process as telescope tracking.

4. Discussion and conclusion

In this paper a preliminary theoretical study of the introduction of a neural network in an Alt-Az telescope axes control system has been presented. The well known self-adaptation and generalization capabilities of such a tool are useful to improve the entire system performance and to add more versatility to the VSPI control structure, especially when the VSPI is not able to give the best correction in real time (in presence of wind disturbance). The adaptation level of the entire system will be sensitively increased, not only as regards the instantaneous position error trend, but also as to the work phase transition, avoiding problems concerning unexpected high noise and actuators saturation. This capability, also, will dynamically assure the best control performance during both pointing and tracking phases. The choice of a MLP model is not a fixed constraint. Radial basis functions (RBFs) and recurrent models are also adequate. In

Table 3
NVSPI vs. VSPI altitude axis tracking performance at different estimated site wind speed percentage

V (m/s)	Night time% (with wind speed $>V$)	RMS tracking error (arcsec) (VSPI model)	RMS tracking error (arcsec) (NVSPI model)
3	77	0.02	0.005
6	50	0.10	0.03
9	24	0.30	0.09
12	11	0.54	0.16
15	5	0.80	0.26
18	2	1.10	0.38

particular RBFs seem to be effective models when input space is not too large, (Alessandri, Sanguineti, Zoppoli, & Parisini, 1996). Their use will be object of future improvements. For a telescope of the class of the VST usually the maximum admitted tracking RMS error is about 0.15 arcsec, a value which does not affect the image quality even in good seeing conditions, because the arcsec/pixel resolution is 0.21. According to this simulation results, the disturbance effect would increase with wind speed as foreseen, especially for the VSPI control scheme; in the NVSPI, with $\alpha = 0.63$ case, up to 12 m/s the effect could be considered not really performance limiting, while at higher wind speeds, also in good seeing conditions, a negative effect could be noticed in both VSPI and NVSPI control models, Table 3.

However, the problem can be limited to a low percentage of telescope usage time; the wind speed, as already stated, is above 12 m/s in about 11% of the time, above 15 m/s only in the 5% of the time. During the most windy nights, in principle it is possible to re-schedule the less performance demanding observation programs, e.g. engineering tests on the telescope and its instrumentation.

References

Alessandri, A., Sanguineti, M., Zoppoli, R., & Parisini, T. (1996). *Neural nonlinear controllers and observers: Stability results. Proceedings of the Eighth Italian Workshop on Neural Nets, WIRN Vietri 96, Vietri sul Mare, Salerno, Italy*, pp. 80–90, May 23–25.

Mancini, D., Brescia, M., Cascone, E., & Schipani, P. (1997). A variable structure control law for telescopes pointing and tracking. In M. Masten (Ed.), *Acquisition, pointing and tracking. Proceedings of SPIE 3086*.

Miller, W. T., Sutton, R. S., & Werbos, P. J. (1990). *Neural networks for control*. Cambridge, MA: MIT Press.

Schipani, P. (2002). *VST project: Telescope dynamic analysis* (*Vol. 4837, Nr. 41*). *Proceedings of SPIE International Congress of Astronomoical Telescopes and Instrumentation, Waikola Hawaii USA*, August 22–28.

Schipani, P., Brescia, M., Mancini, D., Marty, L., & Spirito, G. (2001). *The VST telescope control software in the ESO VLT environment. Proceedings of ICALEPCS, Eighth International Conference on Accelerator and Large Experimental Physics Control Systems, San Jose California USA*, November 27–30, Astro-Ph 0111139.